Robust Multi-signal Estimation Framework with Applications to Inertial Sensor Stochastic Calibration

Robust Multi-signal Estimation Framework with Applications to Inertial Sensor Stochastic Calibration

Chrysostomos Minaretzis[1], Davide A Cucci[1], Naser El-Sheimy[1], Michael G Sideris[1], Stéphane Guerrier[1], and Maria-Pia Victoria-Feser[1]

[1]Affiliation not available

January 26, 2024

Abstract

The stochastic calibration of low-cost and consumer grade inertial sensors has recently become very important due to their wide-spread utilization in a multitude of mass-market applications like smartphone and drone navigation. The reason behind this is because if accurate stochastic modeling about the inertial sensor noise is obtained, then the estimation quality of the navigation solution may improve significantly. Generally, the mainstream methods for stochastic calibration consider only a single signal, collected under static conditions, to infer that knowledge. However, it has been observed that even though the stochastic model structure that characterizes each (static) calibration signal remains the same, its parameter values vary from one replicate to another. Even though techniques have been recently proposed to address this in a statistically efficient way, a very important factor has been neglected, namely the influence of outliers on the estimation process. In this paper, a robust multi-signal framework for the stochastic modeling of inertial sensor errors is proposed, which contains two layers of robustness: one that reduces the influence of outliers in each observed signal (data corruption) and one that safeguards the estimation process from the collection of calibration signal replicates with notably different stochastic behaviour compared to the majority (sample contamination). Furthermore, two estimators are defined from this framework, with each encompassing either one or both layers of robustness, and their efficiency in different data contamination scenarios is assessed in a simulation setting. Finally, real data collected from a consumer-grade MEMS-based device are used within a navigation simulator to evaluate the relationship between the quality of the stochastic models obtained by the two robust estimators in different data collection scenarios and the navigation solution stability.

Robust Multi-signal Estimation Framework with Applications to Inertial Sensor Stochastic Calibration

Chrysostomos Minaretzis, Davide A. Cucci, Naser El-Sheimy, Michael G. Sideris,
Stéphane Guerrier and Maria-Pia Victoria-Feser

Abstract—**The stochastic calibration of low-cost and consumer-grade inertial sensors has recently become very important due to their wide-spread utilization in a multitude of mass-market applications like smartphone and drone navigation. The reason behind this is because if accurate stochastic modeling about the inertial sensor noise is obtained, then the estimation quality of the navigation solution may improve significantly. Generally, the mainstream methods for stochastic calibration consider only a single signal, collected under static conditions, to infer that knowledge. However, it has been observed that even though the stochastic model structure that characterizes each (static) calibration signal remains the same, its parameter values vary from one replicate to another. Even though techniques have been recently proposed to address this in a statistically efficient way, a very important factor has been neglected, namely the influence of outliers on the estimation process. In this paper, a robust multi-signal framework for the stochastic modeling of inertial sensor errors is proposed, which contains two layers of robustness: one that reduces the influence of outliers in each observed signal (data corruption) and one that safeguards the estimation process from the collection of calibration signal replicates with notably different stochastic behaviour compared to the majority (sample contamination). Furthermore, two estimators are defined from this framework, with each encompassing either one or both layers of robustness, and their efficiency in different data contamination scenarios is assessed in a simulation setting. Finally, real data collected from a consumer-grade MEMS-based device are used within a navigation simulator to evaluate the relationship between the quality of the stochastic models obtained by the two robust estimators in different data collection scenarios and the navigation solution stability.**

Index Terms—**Robust Estimation, Inertial Sensor Stochastic Calibration, Generalized Method of Wavelet Moments, Average Wavelet Variance Estimator, Monte-Carlo Simulations, Navigation**

I. INTRODUCTION

A. Calibration Methods

INERTIAL sensors are ubiquitous in modern navigation systems, with applications ranging from space missions, aviation and drones, to smartphone navigation. Their function is to provide high-frequency and short-term precise information on the orientation and velocity change of the platform they are mounted on. Inertial measurements are typically integrated with information from auxiliary sources in order to obtain estimates for the platform position and orientation in 3D space; examples of such sources are the Global Navigation Satellite Systems (GNSS), utilized for strap-down inertial navigation [1] and cameras, used in visual-inertial systems [2].

Like any other sensor, inertial sensors have errors that are both deterministic and stochastic in nature. Deterministic errors such as the stable parts of biases, scale factors and non-orthogonality of the axes can be pre-calibrated and their effects removed from the measurements directly. The additive stochastic part of the errors can only be taken into account "on-flight" within the estimation process in order to serve two main purposes: (i) estimation of the time-correlated part of those stochastic errors in order to remove their influence from the measurements and eventually improve the navigation accuracy [3] and, (ii) estimation of the uncertainty associated with the navigation states, such as position and orientation for the purpose of reliable integrity monitoring. This requires proper modeling of the inertial sensor stochastic errors, a process which is often referred to as "stochastic calibration". This task is generally performed in a black-box fashion on a per-device basis by acquiring static measurements for a long period of time that contain not only the stochastic error itself, but also constant terms such as gravity and the Earth's rotation rate, which can be easily removed. Stochastic calibration of inertial sensors has been widely studied in the last decades and various methods are available for implementing it, ranging from power spectral density analysis [4], [5] to the study of correlation of filtered sensor outputs [6]. The majority of these methods aim to decompose these stochastic signals and/or perform system identification procedures in order to model their behaviour [7], [8].

Modern calibration techniques rely on estimation methods based for example on the Maximum-Likelihood Estimation (MLE) typically obtained through the Expectation–Maximization (EM) algorithm [9]–[11] or, more recently, on the Generalized Method of Wavelet Moments [12] (GMWM). Given a postulated parametric model for the stochastic error $F_{\boldsymbol{\theta}_0}$ that is characterized by the true (unknown) defining parameter vector $\boldsymbol{\theta}_0$ ($\boldsymbol{\theta}_0 \in \boldsymbol{\Theta} \subset \mathbb{R}^p$), the MLE method relies on the likelihood function associated with $F_{\boldsymbol{\theta}_0}$, while the GMWM makes use of the *classical* Wavelet Variance

C. Minaretzis, N. El-Sheimy and M. G. Sideris are with the Department of Geomatics Engineering, University of Calgary, Calgary, Alberta T2N 1N4, Canada. (e-mails: chrysostomos.minaret@ucalgary.ca, elsheimy@ucalgary.ca, sideris@ucalgary.ca)

D. A. Cucci and M.-P. Victoria-Feser are with the Geneva School of Economics and Management, University of Geneva, 1205, Switzerland (e-mails: davide.cucci@unige.ch, maria-pia.victoriafeser@unige.ch).

S. Guerrier is with the Faculty of Science & Geneva School of Economics and Management, University of Geneva, 1205, Switzerland. (e-mail: stephane.guerrier@unige.ch)

(WV) quantity [13] in the context of a moment matching procedure. The GMWM overcomes several limitations of the existing approaches in terms of computational efficiency, numerical stability and statistical consistency (see e.g., [14]).

A major challenge in inertial sensor signal calibration is the determination of the model F_{θ_0} that describes the stochastic error, since possible models are often very complex and consist of composite processes (i.e., the sum of different latent underlying processes). A standard approach for identifying the underlying stochastic processes and estimating their parameters is by using the log-log plot of the Allan Variance (AV) quantity [15], [16], which has been evaluated based on static inertial sensor data so that only the noise is observed. Specifically, by inspecting the shape of the AV in this plot, a decision can be made about the structure of the model F_{θ_0}, while its corresponding parameters are evaluated via independent linear regressions. However, [17] showed that the Allan Variance Linear Regression (AVLR) estimator is inconsistent and unreliable in many cases.

On another note, it is common for Inertial Measurement Unit (IMU) calibration procedures to perform several independent static experimental runs on the same sensor and under the same operating conditions, from which a single signal for calibration is chosen to be used. Therefore, these techniques (e.g., GMWM and AVLR) implicitly assume that the collected data are intrinsically stationary and as such, each collected signal replicate is characterized by the same statistical properties. However, it should be highlighted that a variability in the model parameter values that describe the stochastic behavior of each static run is frequently observed in practice. As a result, this implies that the aforementioned stationarity assumption made by stochastic calibration techniques such as the GMWM and the AVLR is directly compromised.

Given the aforementioned, an alternative calibration method is required, on that is able to take into account the stochastic model parameter variability between experimental runs. To that end, [18], [19] and [20] adopted a mixed-effect modelling approach where the error signals follow a parametric model F_{θ}, where θ is a generic parameter vector of size $(p \times 1)$ such that $\theta \in \Theta \subset \mathbb{R}^p$. In addition, the θ values of that model were considered to be drawn from an unspecified distribution G for each signal realization, thereby accounting for the behavioral variations between them. Standard mixed-effect regression methods aim to estimate the parameters that characterize the distribution G which, in practice, is usually a Gaussian distribution with suitable parameters. On the other hand, [20] proposed a semi-parametric approach tailored to the problem of inertial sensor stochastic calibration which avoids specifying the form of the distribution G. This multi-signal method, called the Average Wavelet Variance (AWV) estimator [20, Section II.B], is capable of optimally estimating parameter values in the sense that they best predict the future behavior of the random parameter θ, and it relies on an optimization problem that only depends on the WV obtained from each run.

B. Motivation

As highlighted in [21], the data employed for stochastic error modeling purposes may contain outliers that can have adverse effects on the estimation process by impacting both the computation of the WV (or AV) quantity that is used for model identification as well as the model parameter estimation. Specifically, those effects can distort the WV (or AV) curve shape and lead to wrong decisions in the model structure identification and to biased parameter estimates. This phenomenon is especially apparent in the case of low-cost and consumer-grade MEMS-based inertial sensors, whose measurements are oftentimes contaminated with outliers, possibly due to the properties of the IMU (e.g., device integrity, material quality, ageing) or the condition of the surface where the IMU has been placed for the calibration data collection (i.e., vibrations). Moreover, the operating conditions, such as the temperature and platform dynamics, have also been found to be an influencing factor to the inertial sensor noise characteristics [22], [23]. Finally, it should be highlighted that the aforementioned AVLR method, despite its wide-spread use, does not contain any features in its algorithm that can provide protection against the influence of outliers.

In [21], a Robust GMWM (RGMWM) framework was proposed, providing an estimator that is far less influenced by the potential presence of outliers in the data, and allows the parameter estimation of stochastic error models in a computationally efficient way. Hence, the RGMWM, which is based on the computation of *robust* WVs, is a useful alternative to other robust estimators (for a general account of robust inferential approaches and motivating examples, see [24], [25]). Nevertheless, the RGMWM is limited to studying the stochastic error behaviour of an inertial sensor using single experimental run. Therefore, if its concept is to be integrated with the multi-signal approach, robustness has to be extended in order to account for data corruption in each collected calibration signal replicate and thus, prevent biased estimations. On top of that, we noticed that in practice, there is a strong likelihood of sample contamination, which can be detected through a comparison of the WVs that correspond to the available signals. As for the signals that constitute this sample contamination, henceforth, we shall refer to them as "abnormal". An example of such an phenomenon is given in Fig. 1, where the classical and robust WV of 6 static accelerometer signal replicates, collected under the same conditions, are displayed. Based on that figure and the classical WVs, replicate no.4 can safely be classified as an abnormal signal since it deviates considerably from the spread of the majority for the mid and higher scales. And, even though the robust WV manages to attenuate that difference for the mid-scales (strong indication of the existence of outliers), the same cannot be said for the higher ones, which is a fact that might create an issue to the stochastic modeling process.

C. Main Contributions

In order to develop a robust multi-signal stochastic analysis framework that has limited sensitivity to data corruption within each experimental run, as well as to sample contamination, we
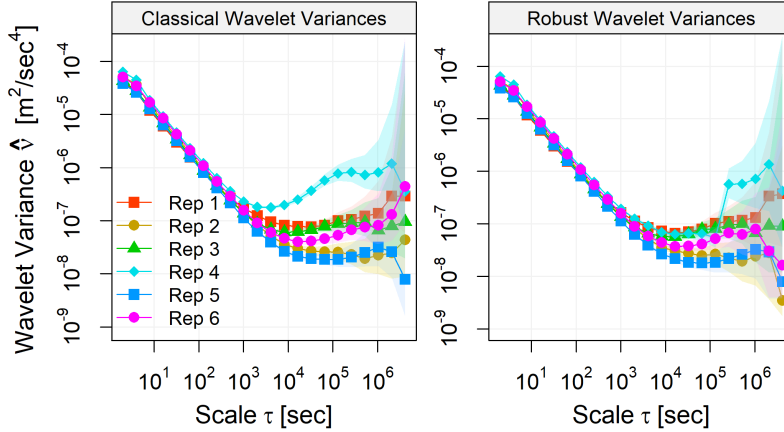
FIG. 1: *Classical (right panel) and robust (left panel) WV (m^2/sec^4) as a function of the scales τ (sec) in a log-log plot*

chose to utilize the AWV estimator. However, its development is not straightforward. In fact, one might be tempted to believe that the augmentation of the AWV estimator with such robust features can be naturally obtained by replacing the classical WV with its robust analogue proposed for example in [21] (see also [26]) and by employing the trimmed mean concept in the evaluation of the characteristic WV used for inference by the AWV. Unfortunately, it turns out that this simple course of action does not directly guarantee the robustness properties of the resulting estimator, which can be shown by means of the Influence Function (IF) [27] that measures the *infinitesimal* robustness property of an estimator.

In this work, we derive the IF (such that IF : $\mathbb{R}^p \mapsto \mathbb{R}^p$) for a general class of estimators, which then allows us to propose a stochastic calibration method that incorporates robust features while considering multiple signals. Specifically, by studying that IF, the quantities of the AWV that need to be bounded in order to ensure the (two-front) robustness of the resulting estimator can be determined. Moreover, we present the conditions under which the statistical consistency of the derived estimator is secured. Finally, we show that its reduced statistical efficiency compared to the classical AWV is quite negligible, while the additional computational effort is also quite small.

From that general framework, we define two estimators: the Singly Robust AWV (SR-AWV) that contains protection against data corruption and the Doubly Robust AWV (DR-AWV), which reinforces robustness against sample contamination as well. In fact, the former can be thought of as a special case of the latter.

In the multi-signal approach, ideally, we expect the WV curves to be close to each other, from which a mean WV can be retrieved that is representative of the sensed behaviour. However, the possible existence of data corruption and sample contamination will inevitably lead to a mean WV that does not realistically describe the available information. Hence, the innovation of the new method is that it ensures that the mean WV used for inference expresses a pragmatic image of the sensed behaviour and thus safeguard not only the model parameter estimation quality but also the proper model structure selection. On another note, and as shown in Fig. 1,

it is possible that the robust WV of the outlying replicate to still present an abnormal behaviour at a certain location of the spectrum, while being logical and among the majority spread at another. Therefore, the advantage offered by the DR-AWV over the SR-AWV in this case is that it manages to simultaneously reduce the influence of that outlying signal to the estimation and consider any useful information that it might contain for other regions of the error spectrum. Finally, the prowess of the new robust multi-signal estimators is not only established in terms of model parameter estimation efficiency, but also in terms of contribution to the INS/GNSS navigation solution under different data contamination scenarios, where the attributes of each estimator can be highlighted compared to the classical *non-robust* approach.

To present the proposed approach, confirm its efficiency in a simulation and a case study setting and discuss the derived results, this paper is organized as follows. In Section II, the proposed robust multi-signal stochastic modeling framework is mathematically defined and proofs about its statistical properties (i.e., robustness, consistency) are provided. With these in mind, Section III evaluates via simulation studies, the benefits of estimators derived by our new robust multi-signal framework to the model parameter estimation efficiency in different data contamination (outlier) settings. In turn, Section IV utilizes real data within a recently proposed navigation simulator (see [28]) in order to investigate the impact of the quality of the derived stochastic modeling knowledge about the inertial sensor random errors to the INS/GNSS navigation performance, when using the new robust multi-signal framework in different outlier scenarios of the real calibration datasets. Finally, Section V contains the conclusions derived from the previous sections.

II. MULTI-SIGNAL ROBUST CALIBRATION

A. Stochastic Framework

We define the i-th discrete-time stochastic signal (i.e., random variable) as $\left(X_t^{(i)}\right) \sim F_{\vartheta_i}$, for $i \in \{1, \ldots, K\}$ being the number of observed signals and with $t = 1, \ldots, T_i$ representing the sample size, while $\vartheta_i \in \Theta \subset \mathbb{R}^p$ (hereinafter an alternative notation for $\boldsymbol{\theta}$) is a realization of the random

variable $\boldsymbol{\vartheta}$ with $\boldsymbol{\vartheta} \overset{iid}{\sim} G$. The distribution $F_{\boldsymbol{\vartheta}_i}$ corresponds to the data-generating process associated with the i-th signal and the distribution G is left unspecified but with the condition $\text{supp}(G) \subseteq \boldsymbol{\Theta}$ being imposed to ensure that the problem is well-defined. Furthermore, we assume that the parameter space $\boldsymbol{\Theta}$ is compact, which ensures that the moments of $\boldsymbol{\vartheta}_i$ (i.e., mean, variance, etc.) are finite. In addition, in order for the stochastic modeling methodology to be applicable, it is assumed that $F_{\boldsymbol{\vartheta}_i}$ is such that $(X_t^{(i)})$ is strictly an intrinsically stationary process, while it is highlighted that the model $F_{\boldsymbol{\vartheta}_i}$ is semi-parametric in the sense that it fully determines the dependence structure of the process over time (through the unknown value $\boldsymbol{\vartheta}_i$) but the distribution of the innovation sequence is left unspecified. Thus, by letting $\mathbf{X}^{(i)} := \left[X_1^{(i)} \ldots X_{T_i}^{(i)} \right]$ we can write

$$\mathbf{X}^{(i)} \big| \boldsymbol{\vartheta}_i \sim \mathcal{F} \left\{ \boldsymbol{\mu}, \boldsymbol{\Sigma}(\boldsymbol{\vartheta}_i) \right\}, \tag{1}$$

where $\mathcal{F}$ denotes a probability distribution, conditional on $\boldsymbol{\vartheta}_i$, in $\mathbb{R}^{T_i}$ with mean $\boldsymbol{\mu}$ and positive definite covariance matrix $\boldsymbol{\Sigma}(\boldsymbol{\vartheta}_i)$.

With this setting in mind, we denote by $\hat{\boldsymbol{\nu}}_i \in \mathbb{R}_+^J$ a suitable estimator for the WV computed based on $\left(X_t^{(i)} \right)$ and with the maximum number of scales J being a *fixed* integer representing the chosen number of WV scales such that $p \leq J < \min_{i=1,\ldots,k} \lfloor \log_2(T_i) \rfloor$. In Sec. II-B, we also impose restriction of $\hat{\boldsymbol{\nu}}_i$ to ensure certain properties of the estimation procedure. Next, we define the expectation of $\hat{\boldsymbol{\nu}}_i$ conditionally on $\boldsymbol{\vartheta}_i$ as $\boldsymbol{\nu}(\boldsymbol{\vartheta}_i) := \mathbb{E}\left[\hat{\boldsymbol{\nu}}_i \big| \boldsymbol{\vartheta}_i \right]$ and thus, we have

$$\boldsymbol{\nu}_0 := \mathbb{E}[\hat{\boldsymbol{\nu}}_i] = \mathbb{E}\left[\mathbb{E}\left[\hat{\boldsymbol{\nu}}_i \big| \boldsymbol{\vartheta}_i \right] \right] = \mathbb{E}[\boldsymbol{\nu}(\boldsymbol{\vartheta}_i)] \neq \boldsymbol{\nu}(\boldsymbol{\mu}_0), \tag{2}$$

where $\boldsymbol{\mu}_0 := \mathbb{E}[\boldsymbol{\vartheta}_i]$ and when $\boldsymbol{\nu}(\boldsymbol{\theta})$ is a non-linear function of $\boldsymbol{\theta}$. Considering this stochastic framework, it may not be optimal to use the parameter vector estimated on the i-th signal to predict the general measurement error of a future signal. As proposed in [20], it would be more appropriate to define a *fixed* parameter vector that adequately represents and predicts the behaviour of all possible signals issued from the stochastic framework, where the parameter values $\boldsymbol{\vartheta}_i$ vary between replicates. In order to do so, [20] defined $\boldsymbol{\theta}_0$ as follows:

$$\boldsymbol{\theta}_0 := \underset{\boldsymbol{\theta} \in \boldsymbol{\Theta}}{\arg\min}\, Q(\boldsymbol{\theta}),$$

where

$$Q(\boldsymbol{\theta}) := \mathbb{E}\left[\| \boldsymbol{\nu}(\boldsymbol{\vartheta}_i) - \boldsymbol{\nu}(\boldsymbol{\theta}) \|_{\boldsymbol{\Omega}}^2 \right], \tag{3}$$

where $\| \mathbf{x} \|_{\mathbf{A}}^2 := \mathbf{x}^T \mathbf{A} \mathbf{x}$ where $\mathbf{x} \in \mathbb{R}^k$ and $\mathbf{A} \in \mathbb{R}^{k \times k}$ and $\mathbb{E}[\cdot]$ denotes the expected value. Furthermore, the vector $\boldsymbol{\nu}(\boldsymbol{\theta})$ of size $(J \times 1)$ (just like $\boldsymbol{\nu}(\boldsymbol{\vartheta}_i)$) represents the theoretical WV implied by the stochastic model $F_{\boldsymbol{\theta}}$ and evaluated at the *fixed* parameter vector $\boldsymbol{\theta}$, while $\boldsymbol{\Omega}$ denotes a positive definite weighting matrix defined in $\mathbb{R}^{J \times J}$.

The criterion in (3) is defined as an expectation under the distribution G whose form however, as underlined earlier, does not need to be specified. Regarding the weighting matrix, for example, one can choose a *fixed* positive definite matrix for $\boldsymbol{\Omega}$ (denoted as $\boldsymbol{\Omega}_0$) or, as discussed in [20], an estimator of the latter matrix (denoted as $\widehat{\boldsymbol{\Omega}}$). As long as this matrix is positive definite and assuming identifiability of the function $\boldsymbol{\nu}(\cdot)$, the criterion in (3) is uniquely minimized in $\boldsymbol{\theta}_0$. With this in mind, the criterion (or loss/objective function) in (3) is an extension of the GMWM objective function that takes into account the internal sensor model G. Therefore, the logic behind choosing this criterion consists of finding a fixed parameter vector $\boldsymbol{\theta}_0$ that minimizes the expected squared-loss between the WV implied by the latter parameter vector and the WV implied by all possible values of the (parameter) random variable $\boldsymbol{\vartheta}_i$. In a Bayesian sense, we are finding the optimal parameter value (according to the GMWM criterion) weighted by the prior distribution G which although not specified, is evaluated empirically through the observed "realizations" or "representations" of the distribution G. In practice, the model $F_{\boldsymbol{\theta}_0}$ can be interpreted as the noise model associated to the WV $\boldsymbol{\nu}(\boldsymbol{\theta}_0)$ which is closest (in the sense of norm defined in (3)) to the expected classical WV $\boldsymbol{\nu}_0$ defined in (2). This interpretation is due to the properties of quadratic forms. Indeed, we have

$$Q(\boldsymbol{\theta}) = \| \boldsymbol{\nu}_0 - \boldsymbol{\nu}(\boldsymbol{\theta}) \|_{\boldsymbol{\Omega}}^2 + \text{tr}\left[\boldsymbol{\Omega} \, \text{var}\left\{ \boldsymbol{\nu}(\boldsymbol{\vartheta}_i) \right\} \right],$$

and, thus, we have

$$\boldsymbol{\theta}_0 = \underset{\boldsymbol{\theta} \in \boldsymbol{\Theta}}{\arg\min}\, Q(\boldsymbol{\theta}) = \underset{\boldsymbol{\theta} \in \boldsymbol{\Theta}}{\arg\min}\, \| \boldsymbol{\nu}_0 - \boldsymbol{\nu}(\boldsymbol{\theta}) \|_{\boldsymbol{\Omega}}^2,$$

since the term $\text{tr}\left[\boldsymbol{\Omega} \, \text{var}\left\{ \boldsymbol{\nu}(\boldsymbol{\vartheta}_i) \right\} \right]$ is not a function of $\boldsymbol{\theta}$. Next, we provide an example that illustrates the difference between our target $\boldsymbol{\theta}_0$ and the expected value of $\boldsymbol{\vartheta}_i$, i.e., $\boldsymbol{\mu}_0$.

EXAMPLE 1: *For $i \in \{1, \ldots, K\}$ and $0 < b < 0.5$, we assume that $\vartheta_i \overset{iid}{\sim} \mathcal{U}(0, b)$, i.e., a uniform distribution between 0 and b. Let $\varepsilon_t^{(i)}$ be an iid sequence such that $\mathbb{E}[\varepsilon_t^{(i)}] = 0$ and $\text{var}(\varepsilon_t^{(i)}) = 1$. Then, we define the following first-order moving-average process:*

$$X_t^{(i)} = \vartheta_i \varepsilon_{t-1}^{(i)} + \varepsilon_t^{(i)}.$$

Under standard regularity conditions, the theoretical WV at the first scale of such process (conditionally on θ) is given by

$$\nu_1(\theta) = \frac{\theta^2 - \theta + 1}{2},$$

Thus, we have

$$\mu_1 = \mathbb{E}[\nu_1(\vartheta)] = \frac{1}{2}\left(\frac{b^2}{3} - \frac{b}{2} + 1 \right).$$

Considering only the first scale, we have

$$\theta_0 = \underset{\theta \in [0, 0.5]}{\arg\min}\, \mathbb{E}\left[\{ \nu_1(\vartheta) - \nu_1(\theta) \}^2 \right]$$
$$= \underset{\theta \in [0, 0.5]}{\arg\min}\, \{ \mu_1 - \nu_1(\theta) \}^2,$$

and we obtain

$$\theta_0 = \frac{1}{2} - \sqrt{\frac{b^2}{3} - \frac{b}{2} + \frac{1}{4}} \neq \mu_0 = \mathbb{E}[\vartheta] = \frac{b}{2}.$$

B. Robust Estimation Procedure

Considering the stochastic framework defined in the previous section, a doubly robust estimator for $\boldsymbol{\theta}_0$ is proposed here. For this purpose, we define the following estimator

$$\hat{\boldsymbol{\theta}} := \operatorname*{argmin}_{\boldsymbol{\theta} \in \boldsymbol{\Theta}} \, \widehat{Q}(\boldsymbol{\theta}), \qquad (4)$$

where

$$\widehat{Q}(\boldsymbol{\theta}) := \Big\| \sum_{i=1}^{K} w_i \boldsymbol{\rho}\left(\hat{\boldsymbol{\nu}}_i, \boldsymbol{\theta}\right) \Big\|_{\boldsymbol{\Omega}}^2, \qquad (5)$$

and where the function $\boldsymbol{\rho} : \mathrm{I\!R}_+^J \times \boldsymbol{\Theta} \mapsto \mathrm{I\!R}^J$ is a suitable function chosen to ensure the robustness properties of the estimated parameter vector $\hat{\boldsymbol{\theta}}$ (such that $\hat{\boldsymbol{\theta}} \in \boldsymbol{\Theta} \subset \mathrm{I\!R}^p$). A simple but arguably non-robust choice of $\boldsymbol{\rho}$ is given by the formula $\boldsymbol{\rho}(\hat{\boldsymbol{\nu}}_i, \boldsymbol{\theta}) = \hat{\boldsymbol{\nu}}_i - \boldsymbol{\nu}(\boldsymbol{\theta}) = [\hat{\nu}_{ij} - \nu_j(\boldsymbol{\theta})]_{j=1,\ldots,J}$. In fact, this choice was considered in [20] which proposed a non-robust version of $\hat{\boldsymbol{\theta}}$. The weights w_i are defined as

$$w_i := d_i \frac{T_i}{\sum_{j=1}^{K} T_j},$$

where d_i is a signal-specific constant such that $\sum_{i=1}^{K} w_i = 1$ and $\sum_{i=1}^{K} w_i \boldsymbol{\rho}\left(\hat{\boldsymbol{\nu}}_i, \boldsymbol{\theta}\right) \xrightarrow{p} \mathbb{E}_G\left[\boldsymbol{\rho}\left(\boldsymbol{\nu}, \boldsymbol{\theta}\right)\right]$. The constants d_i are defined by the user to give more weight to certain signals based on prior knowledge (one would however commonly choose $d_i = 1/K$ for all i). As previously mentioned, the estimator $\hat{\boldsymbol{\nu}}_i$ is a consistent and potentially robust estimator of the WV.

The estimator $\hat{\boldsymbol{\theta}}$ defined in (4), specified through the function $\widehat{Q}(\boldsymbol{\theta})$, can be biased if, in particular, the distributional assumptions for the stochastic signal $(X_t^{(i)})$, i.e. $(X_t^{(i)}) \sim F_{\boldsymbol{\vartheta}_i}$ do not hold exactly. Moreover, in our context, outlying points can also take the form of values for $\boldsymbol{\vartheta}_i$ that can be considered as "extreme" given the values of the majority of the others. The fundamental goal of robust statistics is to provide alternative estimators that have a bounded (asymptotic) bias due to the presence of an infinitesimal quantity of outlying points in the available data (see e.g., [29]). An (indirect) measure of the (maximal) asymptotic bias of potential data contamination is provided by the IF (see [27] and [30] for the time series adaptation) which assesses the effect on the estimator of considering a data generating process in a neighborhood of the targeted model. A robust estimator is then an estimator with a (sufficiently) bounded IF[1]. Intuitively, a bounded IF, hence robust, estimator can be obtained by considering in (5), the following function

$$\sum_{i=1}^{K} w_i \boldsymbol{\rho}\left(\hat{\boldsymbol{\nu}}_i, \boldsymbol{\theta}\right) = \sum_{i=1}^{K} w_i \left[\omega_{ij}(\hat{\nu}_{ij})\hat{\nu}_{ij} - \nu_j(\boldsymbol{\theta}) \right]_{j=1,\ldots,J}$$

$$= \left[\sum_{i=1}^{K} w_i \rho_j\left(\hat{\nu}_{ij}, \nu_j(\boldsymbol{\theta})\right) \right]_{j=1,\ldots,J} \qquad (6)$$

with $\hat{\nu}_{ij}$ a robust estimator of the WV at scale j for series i, and $\omega_{ij}(\hat{\nu}_{ij})$ are such that $\sum_{i=1}^{K} \omega_{ij}(\hat{\nu}_{ij}) = 1, \forall j = 1, \ldots, J$.

While a robust estimator for the WVs ensures that the effect of outlying observations in a series is limited, a weighted mean that downweights the most extreme WV robust estimates within the same scale, bounds the effect of outlying values for a few $\boldsymbol{\vartheta}_i$.

To verify if an estimator has a bounded (asymptotic) bias due to the presence of an infinitesimal quantity of outlying points in the available data, one formalizes the data generating process as a mixture between the hypothetical model (the targeted model) and an arbitrary data contamination process. Formally and generally, let us define ε_X as the contamination level and let (X_t) be a process generated by a model in a neighborhood of $F_{\boldsymbol{\vartheta}}$, where, for convenience, we omit the subscript i, that is

$$F_{\varepsilon_X} = (1 - \varepsilon_X)F_{\boldsymbol{\vartheta}} + \varepsilon_X \Delta_z, \qquad (7)$$

with small (scalar) $\varepsilon_X > 0$. F_{ε_X} is the standard contamination model with Δ_z the Dirac function at an arbitrary point $z = X_t^\star$. Similarly, for the distribution G of the parameters $\boldsymbol{\vartheta}$ of the different series, we consider the mixture distribution $G_{\varepsilon_{\boldsymbol{\vartheta}}} = (1 - \varepsilon_{\boldsymbol{\vartheta}})G + \varepsilon_{\boldsymbol{\vartheta}} \Delta_{\boldsymbol{z}}$, with small (scalar) $\varepsilon_{\boldsymbol{\vartheta}} > 0$ and with $\Delta_{\boldsymbol{z}}$ the Dirac function at an arbitrary point (vector) $\boldsymbol{z} = \boldsymbol{\vartheta}^\star$. Our estimator can be made robust (in the sense that its IF is bounded) through the choices of the functions $\rho_j\left(\hat{\nu}_{ij}, \nu_j(\boldsymbol{\theta})\right)$ in (6) and the estimators $\hat{\boldsymbol{\nu}}_i$. For the functions ρ_j, $j = 1, \ldots, J$, these requirements are detailed in Assumption A in Section III-A, and for the estimator $\hat{\boldsymbol{\nu}}_i$, the IF of $\hat{\boldsymbol{\theta}}$ is bounded if the $\hat{\nu}_{ij}$ are robust estimators. The requirements in Assumption A are satisfied, for example, if one replaces the weighted mean in (6), with a trimmed mean. Namely, let $2a$ be the number of symmetrically trimmed series i for $\hat{\nu}_{ij}$, and let $k = 1, \ldots, K$ be the index of the order statistics $\hat{\nu}_{[k]j} < \hat{\nu}_{[k+1]j}$, then the weights are defined as

$$\omega_{ij} = \frac{1}{K - 2a} \begin{cases} 1 & \forall k \in \{a+1, \ldots, K-(a+1)\} \\ 0 & \text{otherwise.} \end{cases} \qquad (8)$$

Indeed, by removing a (small) part of the most extreme values for the $\hat{\nu}_{ij}$ for each scale j over the K series, we ensure the conditions in Assumption A[2]. Finally, since the WV estimators must be robust estimators, we can choose the ones proposed by [21].

In what follows, we set $\omega_{ij} = 1/J, \forall i, j$ in (6) for the SR-AWV and for the DR-AWV, we use the weights given in (8).

III. STATISTICAL PROPERTIES

In this section, we first derive the conditions for the proposed estimator in (6) to have a bounded IF. We then also develop the conditions under which a bounded IF estimator is consistent.

---

[1]Indeed, if the support of the estimator is compact, the IF is necessarily bounded, but it can take very large values leading to excessive asymptotic bias. Hence, bounding somehow influential and arbitrary points, limits the size of the bias more effectively.

[2]Actually, the partial derivatives of $\rho_j(\nu_j, \boldsymbol{\theta})$ are bounded if $\rho_j(\nu_j, \boldsymbol{\theta})$ is differentiable and monotone. When using non continuous weights such as the ones for a trimmed mean, this introduces non differentiability at some points ν_j, of nil measure. We could define a continuous weight function to avoid this technical problem, but this would have no incidence in practice, almost surely.

A. Robustness properties

For convenience, and without loss of generality, we set the (fixed) weights in (5) to 1, i.e. $w_i = 1$, $\forall i$. In order to define a robust estimator with a bounded IF we need to set the following conditions.

ASSUMPTION A (Robustness): *Let denote ρ_j the jth element of the function $\boldsymbol{\rho}$ in (5), and suppose it only depends on $\hat{\nu}_{ij}$ and $\nu_j(\boldsymbol{\theta})$ as in (6). Then, there exists a finite positive constant C such that for all $j \in \{1, \ldots, J\}$ and all $l \in \{1, \ldots, p\}$, we have*

$$1) \quad \sup_{\nu_j \in \mathbb{R}_+, \boldsymbol{\theta} \in \boldsymbol{\Theta}} \left\{ \|\rho_j(\nu_j, \boldsymbol{\theta})\|_{\max} \right\} < C,$$

$$2) \quad \sup_{\nu_j \in \mathbb{R}_+, \boldsymbol{\theta} \in \boldsymbol{\Theta}} \left\{ \left\| \frac{\partial}{\partial \theta_l} \rho_j(\nu_j, \boldsymbol{\theta}) \right\|_{\max} \right\} < C, \text{ and}$$

$$3) \quad \sup_{\nu_j \in \mathbb{R}_+, \boldsymbol{\theta} \in \boldsymbol{\Theta}} \left\{ \left\| \frac{\partial}{\partial \nu_j} \rho_j(\nu_j, \boldsymbol{\theta}) \right\|_{\max} \right\} < C.$$

where $\|\mathbf{A}\|_{\max}$ denotes the max of the matrix $\mathbf{A} \in \mathbb{R}^{n \times m}$, i.e., $\|\mathbf{A}\|_{\max} = \max_{i=1,\ldots,n, j=1,\ldots,m} |A_{i,j}|$.

In most instances, 1) implies 2) and 3), as is the case (almost surely[2]) with ρ_j being a weighted average with weights given in (8). However, we keep 2) and 3) for the sake of completeness.

ASSUMPTION B (Stationarity): *For all $i \in \{1, \ldots, K\}$ and conditionally on ϑ_i, we assume that $\left(X_t^{(i)}\right)$ for $j = 1, \ldots, J_i$ and $t = 1, \ldots, T_i$, is a strictly (intrinsically) stationary process.*

The IF is obtained by taking the Gâteaux derivative of the estimator seen as a functional of the mixture distributions (as in (7)) with respect to the contamination level when the later diverges to 0 from the positive side. Indeed, in the data contamination case, $\hat{\boldsymbol{\theta}}$ depends on both distributions $G_{\varepsilon\vartheta}$ and F_{ε_X} while $\hat{\boldsymbol{\nu}}_i$ depend only on the distribution F_{ε_X}, so that $\hat{\boldsymbol{\theta}}$ can be written as a functional of both contaminated distributions as $\hat{\boldsymbol{\theta}}(G_{\varepsilon\vartheta}, F_{\varepsilon_X})$. The IF of $\hat{\boldsymbol{\theta}}$, is then defined as

$$\text{IF}(\boldsymbol{\zeta}^*, \hat{\boldsymbol{\theta}}, G, F_{\vartheta}) = \frac{\partial}{\partial \varepsilon_{\vartheta}} \frac{\partial}{\partial \varepsilon_X} \hat{\boldsymbol{\theta}}(G_{\varepsilon\vartheta}, F_{\varepsilon_X}) \Bigg|_{\varepsilon_X \downarrow 0, \varepsilon_{\vartheta} \downarrow 0} \quad (9)$$

where $\boldsymbol{\zeta}^* = (X_t^*, (\boldsymbol{\vartheta}^*)^T)^T$ with, respectively, X_t^* and $\boldsymbol{\vartheta}^*$ the (arbitrary) contamination points of, respectively, F_{ε_X} and $G_{\varepsilon\vartheta}$. Eq. (9) can also be decomposed as

$$\text{IF}(\boldsymbol{\zeta}^*, \hat{\boldsymbol{\theta}}, G, F_{\vartheta})$$
$$= \left[\frac{\partial}{\partial \varepsilon_{\vartheta}} \frac{\partial}{\partial \varepsilon_X} \hat{\theta}_l(G_{\varepsilon\vartheta}, F_{\varepsilon_X}) \Bigg|_{\varepsilon_X \downarrow 0, \varepsilon_{\vartheta} \downarrow 0} \right]_{l=1,\ldots,p}$$
$$= \left[\text{IF}_l\left((X_t^*, \vartheta_l^*), G, F_{\vartheta}\right) \right]_{l=1,\ldots,p} \quad (10)$$

so that each p elements of the IF need to be bounded for $\hat{\boldsymbol{\theta}}$ to be a robust estimator. As stated in Proposition 1 below, whose detailed proof is given in the supplemental material, the IF of $\hat{\boldsymbol{\theta}}$ defined in (4) and (5), is proportional to the IF of $\hat{\nu}_j$, so that for $\hat{\boldsymbol{\theta}}$ to be robust in the sense of having a bounded IF, the WV $\hat{\nu}_{ij}$ need to be robust estimators. Moreover, the bounds on the IF of $\hat{\boldsymbol{\theta}}$ also depend on the functions $\rho_l(\boldsymbol{\nu}, \theta)$,

so that the IF provides a convenient way to properly define the later in order to obtain a robust estimator for $\boldsymbol{\theta}$.

PROPOSITION 1: *Under Assumptions A and B, and if the IF of $\hat{\nu}_{ij}$ are bounded $\forall i = 1, \ldots, K$, $j = 1, \ldots, J$, the IF of $\hat{\boldsymbol{\theta}}$ defined in (4) is bounded.*

PROOF: Without loss of generality, and for clarity of exposition purposes, we consider that the contamination level ε_X in the contamination model in (7), is the same for all stochastic signals. The estimator $\hat{\boldsymbol{\theta}}$ depends on both empirical distribution associated to G and the F_{ϑ_i} while $\hat{\boldsymbol{\nu}}$ depend on the empirical distribution associated to the F_{ϑ_i}. In the data contamination case, it can be written as $\hat{\boldsymbol{\theta}}(G_{\varepsilon\vartheta}, F_{\varepsilon_X})$. The later is implicitly defined through

$$\widehat{Q}\left(\hat{\boldsymbol{\theta}}(G_{\varepsilon\vartheta}, F_{\varepsilon_X})\right)$$
$$= \left\| \mathbb{E}_{\varepsilon\vartheta}\left[\boldsymbol{\rho}\left(\hat{\boldsymbol{\nu}}(F_{\varepsilon_X}), \hat{\boldsymbol{\theta}}(G_{\varepsilon\vartheta}, F_{\varepsilon_X})\right)\right] \right\|_{\boldsymbol{\Omega}}^2$$
$$= \left\| \mathbb{E}_{\varepsilon\vartheta}\left[\boldsymbol{\varrho}(F_{\varepsilon_X}, G_{\varepsilon\vartheta})\right] \right\|_{\boldsymbol{\Omega}}^2,$$

where $\mathbb{E}_{\varepsilon\vartheta}$ is the expectation taken under $G_{\varepsilon\vartheta}$ and

$$\boldsymbol{\varrho}(F_{\varepsilon_X}, G_{\varepsilon\vartheta}) = \left[\varrho_j(F_{\varepsilon_X}, G_{\varepsilon\vartheta}) \right]_{j=1,\ldots,J}$$
$$= \left[\rho_j\left(\hat{\nu}_j(F_{\varepsilon_X}), \nu_j\left(\hat{\boldsymbol{\theta}}(G_{\varepsilon\vartheta}, F_{\varepsilon_X})\right)\right)\right]_{j=1,\ldots,J}.$$

Let also

$$m\left(\hat{\boldsymbol{\theta}}(G_{\varepsilon\vartheta}, F_{\varepsilon_X})\right) = \widehat{Q}\left(\hat{\boldsymbol{\theta}}(G_{\varepsilon\vartheta}, F_{\varepsilon_X})\right),$$

which is the minimum value of $\widehat{Q}(\boldsymbol{\theta})$. The IF is implicitly defined though the equality between

$$\frac{\partial}{\partial \varepsilon_{\vartheta}} \frac{\partial}{\partial \varepsilon_X} \left\| \left[\mathbb{E}_{\varepsilon\vartheta}\left[\varrho_j(F_{\varepsilon_X}, G_{\varepsilon\vartheta}) \right]\right]_{j=1,\ldots,J} \right\|_{\boldsymbol{\Omega}}^2 \Bigg|_{\varepsilon_X \downarrow 0, \varepsilon_{\vartheta} \downarrow 0} \quad (11)$$

and

$$\frac{\partial}{\partial \varepsilon_{\vartheta}} \frac{\partial}{\partial \varepsilon_X} m\left(\hat{\boldsymbol{\theta}}(G_{\varepsilon\vartheta}, F_{\varepsilon_X})\right) \Bigg|_{\varepsilon_X \downarrow 0, \varepsilon_{\vartheta} \downarrow 0}.$$

We first have that

$$\frac{\partial}{\partial \varepsilon_{\vartheta}} \frac{\partial}{\partial \varepsilon_X} m\left(\hat{\boldsymbol{\theta}}(G_{\varepsilon\vartheta}, F_{\varepsilon_X})\right) \Bigg|_{\varepsilon_X \downarrow 0, \varepsilon_{\vartheta} \downarrow 0}$$
$$= \left[\frac{\partial}{\partial \theta_l} m(\boldsymbol{\theta}) \text{IF}_l\left((X_t^*, \vartheta^*), \hat{\theta}_l, (G, F_{\vartheta})\right)\right]_{l=1,\ldots,p} \quad (12)$$

Given that the IF of $\hat{\boldsymbol{\theta}}$ is bounded if all its p elements are bounded (see (10)), we can derive the IF for each term, i.e. $\text{IF}_l\left((X_t^*, \vartheta^*), \hat{\theta}_l, (G, F_{\vartheta})\right)$ in (10). For (11), after tedious but

straightforward derivations (see the supplemental material for details), and combining with (12), we obtain

$$\left(\sum_{j=1}^{J} H_j\left(\boldsymbol{\nu}, \boldsymbol{\theta}\right) \boldsymbol{M}_4\left(\nu_j, \boldsymbol{\theta}\right) + \frac{\partial}{\partial \theta_l} m(\boldsymbol{\theta}) \right)$$
$$\mathrm{IF}_l\left((X_t^*, \vartheta^*), \hat{\theta}_l, (G, F_{\boldsymbol{\vartheta}})\right)$$
$$= \sum_{j=1}^{J} H_j\left(\boldsymbol{\nu}, \boldsymbol{\theta}\right) \left(\boldsymbol{M}_1\left(\nu_j, \boldsymbol{\theta}\right) + \boldsymbol{M}_3\left(\nu_j, \hat{\boldsymbol{\theta}}\right) \right.$$
$$\left. - \boldsymbol{M}_4\left(\nu_j, \boldsymbol{\theta}\right) \right) \mathrm{IF}\left(X_t^*, \hat{\nu}_j, F_{\boldsymbol{\vartheta}}\right)$$
$$+ \sum_{j=1}^{J} H_j\left(\boldsymbol{\nu}, \boldsymbol{\theta}\right) \left[\left(\boldsymbol{M}_2\left(\nu_j, \boldsymbol{\theta}\right) + \boldsymbol{M}_5\left(\nu_j, \boldsymbol{\theta}\right) \right) \right.$$
$$\left. \mathrm{IF}\left(X_t^*, \hat{\nu}_j, F_{\boldsymbol{\vartheta}}\right) \right] \mathrm{IF}\left(\vartheta^*, \hat{\theta}_l, G\right)$$
$$+ \sum_{j=1}^{J} H_j\left(\boldsymbol{\nu}, \boldsymbol{\theta}\right) \boldsymbol{M}_6\left(\nu_j, \hat{\boldsymbol{\theta}}\right)$$
$$\mathrm{IF}\left(X_t^*, \hat{\theta}_l\left(\vartheta^*, F_{\boldsymbol{\vartheta}}\right), F_{\boldsymbol{\vartheta}}\right) \tag{13}$$

where $H_j\left(\boldsymbol{\nu}, \boldsymbol{\theta}\right)$, $\boldsymbol{M}_1\left(\nu_j, \hat{\boldsymbol{\theta}}\right)$, $\boldsymbol{M}_2\left(\nu_j, \hat{\boldsymbol{\theta}}\right)$, $\boldsymbol{M}_4\left(\nu_j, \hat{\boldsymbol{\theta}}\right)$ and $\boldsymbol{M}_5\left(\nu_j, \hat{\boldsymbol{\theta}}\right)$ are quantities that do not depend on the data, while

$$\boldsymbol{M}_3\left(\nu_j, \hat{\boldsymbol{\theta}}\right) = \frac{\partial}{\partial \nu_j} \rho_j\left(\nu_j, \hat{\boldsymbol{\theta}}\left(\vartheta^*, F_{\boldsymbol{\vartheta}}\right)\right)$$
$$\boldsymbol{M}_6\left(\nu_j, \hat{\boldsymbol{\theta}}\right) = \frac{\partial}{\partial \theta_l} \rho_j\left(\nu_j, \boldsymbol{\theta}\right)\Big|_{\boldsymbol{\theta}=\hat{\theta}(\vartheta^*, F_{\boldsymbol{\vartheta}})}$$

are data contamination dependent, but are bounded if conditions 2) and 3) in Assumption A hold. From (13), one can deduce that the IF of the lth element of $\hat{\boldsymbol{\theta}}$, $\mathrm{IF}_l\left((X_t^*, \vartheta^*), \hat{\theta}_l, (G, F_{\boldsymbol{\vartheta}})\right)$, is bounded if $\mathrm{IF}\left(X_t^*, \hat{\nu}_j, F_{\boldsymbol{\vartheta}}\right), \forall j = 1, \ldots, J$, $\mathrm{IF}\left(X_t^*, \hat{\theta}_l\left(\vartheta^*, F_{\boldsymbol{\vartheta}}\right), F_{\boldsymbol{\vartheta}}\right)$, and $\mathrm{IF}\left(\vartheta^*, \hat{\theta}_l, G\right)$ are bounded. We have that $\mathrm{IF}\left(X_t^*, \hat{\nu}_j, F_{\boldsymbol{\vartheta}}\right), \forall j = 1, \ldots, J$ is bounded by the conditions in Proposition 1, which implies that $\mathrm{IF}\left(X_t^*, \hat{\theta}_l\left(\vartheta^*, F_{\boldsymbol{\vartheta}}\right), F_{\boldsymbol{\vartheta}}\right)$ is bounded if $\mathrm{IF}\left(\vartheta^*, \hat{\theta}_l, G\right)$ is bounded. For the later, after tedious but straightforward derivations (see the supplemental material for details), we obtain that it is bounded if condition 1) in Assumption A is satisfied. $\square$

B. Consistency

From (6), we can express $\hat{\boldsymbol{\theta}}$ as

$$\hat{\boldsymbol{\theta}} = \underset{\boldsymbol{\theta} \in \boldsymbol{\Theta}}{\arg\min} ||\bar{\boldsymbol{\nu}} - \boldsymbol{\nu}(\boldsymbol{\theta})||_{\Omega}^2$$

with

$$\bar{\boldsymbol{\nu}} = \left[\sum_{i=1}^{K} w_i \omega_{ij}(\hat{\nu}_{ij}) \hat{\nu}_{ij} \right]_{j=1,\ldots,J}. \tag{14}$$

Following [31], for consistency of $\hat{\boldsymbol{\theta}}$, and by using $\xrightarrow{p}$ to denote convergence in probability, we need

$$||\bar{\boldsymbol{\nu}} - \boldsymbol{\nu}(\theta)||_{\Omega}^2 \xrightarrow{p} ||\mathbb{E}[\bar{\boldsymbol{\nu}}] - \boldsymbol{\nu}(\theta)||_{\Omega}^2$$

with $\mathbb{E}[\bar{\boldsymbol{\nu}}] = \boldsymbol{\nu}_0$, which, by the continuous mapping theorem and for any consistent estimator $\hat{\nu}_{ij}$, is achieved if Assumption C below is satisfied.

ASSUMPTION C: $\bar{\boldsymbol{\nu}}$ *defined in* (14) *is such that*

$$\bar{\boldsymbol{\nu}} \xrightarrow{p} \boldsymbol{\nu}(\boldsymbol{\theta}_0) = \boldsymbol{\nu}_0.$$

Under some technical requirements (see [21] for details), we have that that the robust $\hat{\boldsymbol{\nu}}$ proposed by [21] is a consistent estimator of $\boldsymbol{\nu}(\boldsymbol{\theta}_0)$. For $\bar{\boldsymbol{\nu}}$ to be consistent, we need to impose some additional conditions. Recall that we propose for $\bar{\boldsymbol{\nu}}$ a trimmed mean (see (8)) with a given trimming proportion a such that $2(a-1)$ is the number of symmetrically trimmed series. For the trimmed mean to be consistent, the trimming proportion should vanish as $K \to \infty$, or, in other terms the number of trimmed series should be fixed $\forall K$. This type of requirement has been used for controlling the estimation bias induced by heavy tail distributions in non parametric settings; see e.g., [32]. Therefore, admitting that outlying series might happen in a non systematic fashion, hence not as a constant proportion, and letting the proportion $a \to 0$ in (8), $\bar{\boldsymbol{\nu}}$ is a consistent estimator of $\boldsymbol{\nu}(\boldsymbol{\theta}_0)$, which implies that $\hat{\boldsymbol{\theta}}$ is a consistent estimator of $\boldsymbol{\theta}_0$.

IV. SIMULATION STUDY

The purpose of this section is to highlight the effectiveness of the new robust estimators against their classical version in targeting the true (unknown) model parameter values that describe the stochastic error behaviour of low-cost and consumer-grade inertial sensor measurements. To accomplish this, a simulation study is conducted for the following data collection scenarios, based on typical accelerometer measurements:

1) outlier-free (clean setting - Scenario I),
2) various types of outliers (step function, random point replacement with white noise, vibrations) are introduced to the replicates (data corruption setting - Scenario II),
3) the signal replicate distribution of the former setting is modified by including a signal with significantly different stochastic error behaviour compared to the rest (sample contamination setting - Scenario III).

In addition, the statistical performance evaluation of the aforementioned estimators in each simulation setting is conducted by utilizing a robust version of the Root Mean Square Error (RMSE) given by the following formula [21]:

$$\mathrm{RMSE} = \sqrt{\mathrm{med}\left(\frac{\hat{\theta}_l - \theta_{l,o}}{\theta_{l,o}}\right)^2 + \mathrm{mad}\left(\frac{\hat{\theta}_l}{\theta_{l,o}}\right)^2}, \tag{15}$$

where $\mathrm{med}(\cdot)$ is the median operator, $\mathrm{mad}(\cdot)$ is median absolute deviation operator, $\hat{\boldsymbol{\theta}}_l, l = 1, \ldots, p$ is the vector of

estimates obtained by simulations for the l-th element of $\boldsymbol{\theta}$, and $\theta_{l,o}$ is the corresponding true parameter value (scalar). As for the reason why such metric was selected, it is to allow for a more meaningful comparison between the classical and robust estimators, since the former's bias is unbounded in the presence of outliers.

Assuming $K = 8$ signal replicates of length $T = 524284$ samples (approx. 1.5 hrs) apiece and with data interval $f = 100$ Hz are produced from a composite stochastic model, say the N_1, via Monte-Carlo (MC) simulations. Specifically, N_1 consists of one Autoregressive process of order 1 (AR1), one Random Walk (RW) and one White Noise (WN) process, while their parameter values that characterize each replicate are realizations that are randomly drawn from the following beta (β) distributions:

- $AR1(\phi)$ with $\phi = 0.9835489 + B_1 \cdot 3.4476489 \cdot 10^{-3}$, $B_1 \sim \beta(6, 2)$
- $AR1(\eta^2)$ with $\eta^2 = 1.286053 \cdot 10^{-8} + B_2 \cdot 9.019592 \cdot 10^{-9}$, $B_2 \sim \beta(2.2, 6.1)$
- $RW(\gamma^2)$ with $\gamma^2 = 2.904098 \cdot 10^{-11} + B_3 \cdot 1.279669 \cdot 10^{-11}$, $B_3 \sim \beta(1.8, 3.5)$
- $WN(\sigma^2)$ with $\sigma^2 = 5.195192 \cdot 10^{-5} + B_4 \cdot 5.24353 \cdot 10^{-6}$, $B_4 \sim \beta(3, 4)$

The produced "clean replicates", representing Scenario I, are utilized to perform the multi-signal stochastic analysis using the AWV, SR-AWV and DR-AWV estimators and eventually estimate the N_1 model parameter values. Furthermore, it is noted that the classical WV (based on the input data) used by the classical AWV estimator is

$$\bar{\boldsymbol{\nu}} = \left[\sum_{i=1}^{K} w_i \hat{\nu}_{ij} \right]_{j=1,\ldots,J} \tag{16}$$

and that for the DR-AWV estimator, a 30% trim (4 replicates are removed in total) is chosen to be used. The aforementioned steps are repeated for $H = 500$ times and based on the results, the RMSE quantity is calculated, with the true parameter values being determined via parametric bootstrap. In fact, as shown in (2), the expected values of each parameter taken separately would not have been suitable.

As for Scenario II, realistic outliers are introduced to each signal replicate. Specifically, a step function centered in the middle of the signal with amplitude $A = 0.002 \ m/sec^2$ is added to the entirety of each signal, 131 points (0.025% of the total signal length) are randomly chosen and replaced by Gaussian WN characterized by $\sigma^2 = 0.02$ and five small vibrations (500 data points each) every 90000 samples are added to three of the available signal replicates. Subsequently, the three estimators under analysis are used to estimate the N_1 model parameters and evaluate the RMSE value for each of them.

Regarding Scenario III, it contains the same kind and magnitude of outliers as Scenario II. In addition, a replicate to which no vibrations are to be added is chosen and its RW parameter realization is multiplied by a factor of 4 in every simulation. In this way, as illustrated in Fig. 1, the case where an abnormal replicate has been collected is realistically emulated. Eventually, the classical and robust multi-signal estimators are employed for the estimation of the N_1 defining parameters and the respective RMSE quantity for each of them is calculated.

With the RMSE results from the above operations in mind, Fig. 2, a semi-log plot w.r.t the y-axis is created, where the behavior of the statistical metric can studied. By inspection, it is evident that the classical and robust estimators have an almost equivalent performance in the case where available data contain no outliers (Scenario I). As a result, the new robust estimators can be safely used in the clean data setting instead of the classical AWV without any meaningful loss in efficiency. In fact, this also means that the conclusions derived by [33] for the single-signal case can be extended to the multi-signal approach as well. Moreover, with respect to Scenario II, the classical estimator appears to be considerably biased compared to the robust ones, which are not only equivalent to each other but they also manage to maintain their efficiency at the same levels as in the clean scenario. Finally, regarding Scenario III, it is apparent that the existence of the abnormal replicate has considerably degraded the efficiency of the AWV and SR-AWV estimators for the RW parameter, something that is reasonable, given the manner in which it was constructed. As for the DR-AWV, it seems that it has managed to successfully avoid its harmful influence.

V. CASE STUDY

In the previous section, we studied the performance of the two new robust multi-signal estimators in different scenarios with regards to model parameter estimation statistical efficiency. However, it is not at all clear what the impact of this stochastic modeling information in each scenario would be to the final navigation performance, something that has not been meticulously investigated in the literature.

An insight to that influence could be provided through the use of the navigation simulator[3] proposed in [28]. This is a framework that it is not only able to reproduce the *perfect* INS measurements as well as the GNSS information (i.e., position and velocity), given a reference trajectory, but also to realistically simulate their respective noises during the movement, based on real static inertial data for the INS system and on the user's specifications for the GNSS one. In addition, the simulator performs the INS/GNSS integration by means of the Extended Kalman Filter (EKF) and provides the capability to calculate statistical metrics (i.e., navigation state estimation accuracy, mean position error, mean orientation error, empirical coverage). Through these quantities, as demonstrated in [28], it is possible to assess the INS performance in terms of the stochastic model choice for the inertial sensor errors. Therefore, in this section, we will be utilizing real inertial sensor calibration signal replicates, perform their stochastic analysis in different contamination scenarios using the AWV, SR-AWV and DR-AWV estimators and eventually determine the nature of the correlation between stochastic calibration efficiency and INS navigation performance in each of those scenarios respectively.
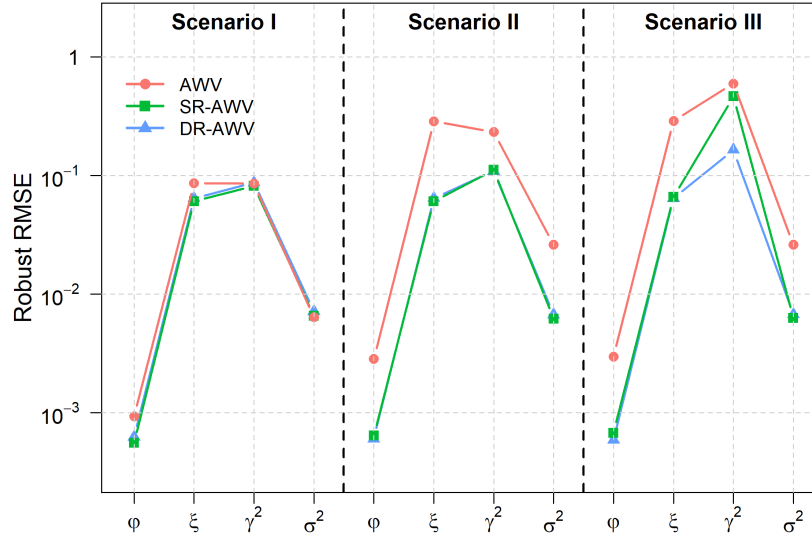
---

[3]Nav simulator "R" package: https://github.com/SMAC-Group/navigation

FIG. 2: *Robust RMSE calculated using* (15), *for the estimators of the* N_1 *parameters* $\phi, \eta^2, \gamma^2, \sigma^2$, *computed on* $H = 500$ *simulated MC samples under Scenario I (no data contamination), Scenario II (data contamination within each replicate), and Scenario III (contamination both within and between replicates) of accelerometer data, using the AWV (dots), SR-AWV (squares) and DR-AWV (triangles) estimators.*

For the purposes of our study here, the reference trajectory that is to be inputted into the simulator was chosen to be a 15-minute land vehicle trajectory derived using NovAtel's high-end Synchronous Position, Attitude and Navigation (SPAN) INS/GNSS integrated system. Specifically, this system is comprised by the tactical grade, low-noise iMAR-FSAS IMU and a GPS/GLONASS high-performance NovAtel receiver, which by means of loosely-coupled integration, was able to provide high accuracy position and attitude information for the whole trajectory shown in Fig. 3 at a 100 Hz rate.
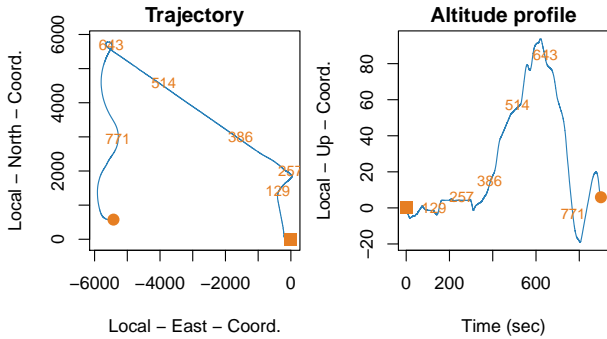
FIG. 3: *Land vehicle reference trajectory on the horizontal (left panel) and vertical plane (right panel) as it was derived from the SPAN system*

As for the calibration inertial data and for the purposes of this experiment, the consumer-grade MEMS-based Xsens MTi-G-710 was chosen to be the source. It was placed on a levelled surface and multiple 1.5hr static datasets at a 100 Hz rate were collected under the same conditions. Then, a comparison between the classical and robust ([21]) WVs was conducted, as a rough indicator for the selection of free-from-outliers replicates. Moreover, the behaviour of the WVs in each of those signals and for each sensor was inspected and it was determined that all three accelerometers present a

very similar behaviour, with the same also applying for the gyroscopes. In the end, with these two criteria in mind, 8 accelerometer and 8 gyroscope signal replicates were chosen as representative for each inertial sensor type (see Fig. 4 for the selected accelerometer signals as an example) and based on which, the stochastic error analysis will be conducted.
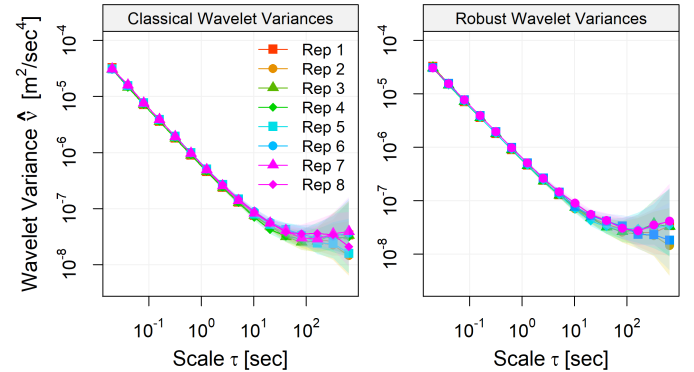

FIG. 4: *Classical (right panel) and Robust empirical WVs (left panel) in* m^2/sec^4, *as a function of the scales* τ *(sec) in a log-log plot, computed on the 8 selected clean accelerometer signal replicates*

It should also be mentioned that apart from these signals, a 9th accelerometer and gyroscope replicate was chosen based on the previously mentioned criteria. The reason behind this choice was to provide the framework with the necessary data in order to generate realistic INS errors during the simulations (see [28] for more information on how exactly this is done). As for the simulated GNSS information that will be used to aid the INS operation, its rate was set to $1Hz$, the horizontal and vertical position errors were assumed to be defined by WN with variances equal to 4 and $16m^2$ respectively, while the horizontal and vertical velocity errors were characterized by WN with variances equal to 0.0016 and 0.0036 m/sec^2.

The final step, before running the simulations, is to define

the three different data contamination scenarios, just like we did in Section IV, and perform the stochastic analysis for each of them. Therefore, regarding Scenario I, represented by the previously selected clean signal replicates, it was identified that the classical WV utilized by the AWV estimator (henceforth referred to as WV-AWV) and the robust WV ([21]) utilized by the SR-AWV and DR-AWV estimators (henceforth referred to as WV-SR-AWV and WV-DR-AWV respectively), present a very similar behaviour. Moreover, it was also found that the model N_2 comprised by the addition of two AR1s, one RW, one WN and one Quantization Noise (QN) process is able to describe both sensor types, the fit of which is shown in Fig. 5 for the accelerometer data using the AWV estimator.
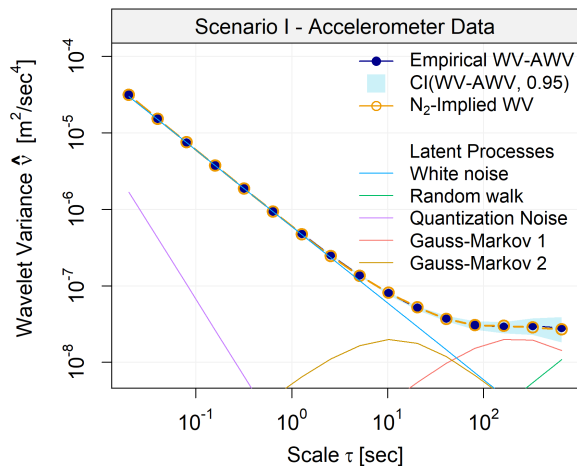
FIG. 5: *Empirical WV-AWV* (16) *in* m^2/sec^4, *along with associated 95% confidence interval and Implied WV constructed from the parameters of the fitted* N_2 *model. Also, the individual contribution of each latent process to the Implied WV is drawn*

As for Scenario II, its creation required that both the accelerometer and gyroscope data to be compromised by three different types of outliers as shown below:

1) point replacement with WN: 1% of each signal is randomly selected and replaced by WN with mean equal to the sample mean of the signal and standard deviation equal to 0.16 m/sec^2 for the accelerometer replicates and 0.026 rad/sec for the gyroscope ones
2) 5 vibrations of 500 points length every 90000 samples were added to both types of signals
3) a step function centered in the middle of each signal is added to them, with an amplitude $A_{accel(1,...,8)} = $ 0.0041, 0.0032, 0.0055, 0.0045, 0.0034, 0.0060, 0.0061, 0.0030 m/sec^2 for the accelerometer and $A_{gyro(1,...,8)} = $ 0.00095, 0.00114, 0.00100, 0.00094, 0.00110, 0.00085, 0.00055, 0.00090 rad/sec for the gyroscope replicates.

After these outliers have been included to the available signal replicates, the WV-AWV, WV-SR-AWV and WV-DR-AWV were calculated and depicted in the left panels of Fig. 6. Based on them, the WV-SR-AWV and WV-DR-AWV are very similar to each other and the WV-AWV appears to have been significantly affected by the introduction of the artificial outliers. Furthermore, it is noticed that the WV-SR-AWV and

WV-DR-AWV manage to stay close to the clean scenario in terms of the lower (WN part) and higher (RW part) scales, while unfortunately, the same cannot be said for the mid ones.

Finally, regarding Scenario III, it is the same as Scenario II but with two replicates, for both the accelerometer and the gyroscope data, presenting a significantly different behaviour compared to the others. The characteristics of the outliers that were used to create such abnormal signals are listed below:

1) data substitution with WN: 5242 samples (1% of each signal's size) were chosen arbitrarily and replaced by data, drawn from a WN process with $\sigma_{accel(3,8)} = $ 0.18 m/sec^2 for the accelerometer and $\sigma_{gyro(2,5)} = $ 0.022, 0.026 rad/sec for the gyroscope signals.
2) 5 small vibrations were introduced, with the same characteristics as in Scenario II
3) a step function with its nonzero section starting after the half-point of the abnormal signals with an amplitude $A_{accel(3,8)} = $ 0.0062, 0.0045 m/sec^2 and $A_{gyro(2,5)} = $ 0.00114, 0.00110 rad/sec for each signal type respectively.
4) a time series with the same size as the available signals was produced based on an AR1 process and added to the data, the properties of which are listed here:
   - $AR1_{accel(3,8)}(\phi = 0.975761, \eta^2 = 3.397832 \cdot 10^{-7})$
   - $AR1_{gyro(2)}(\phi = 0.97239103, \eta^2 = 1.074129 \cdot 10^{-8})$
   - $AR1_{gyro(5)}(\phi = 0.9766580, \eta^2 = 5.313189 \cdot 10^{-9})$

Following the aforementioned adjustments that created Scenario III, the WV-AWV, WV-SR-AWV and WV-DR-AWV were calculated and illustrated in the right panels of Fig. 6. According to them, the WV-DR-AWV estimator remains very close to its Scenario II behaviour, which means that it manages to handle the existence of the abnormal replicates. In addition, we note that the WV-SR-AWV appears to be affected in the mid scales, something that is very logical since the added AR1 process occupies that specific region of the WV scales (mid-frequencies of the signal spectrum).

Using the classical WV of the three multi-signal estimators in each of the three scenarios, the stochastic analysis of the inertial sensor errors is conducted. Having done that, we can now embed the the estimated quantities into the navigation simulator along with the trajectory information and the INS/GNSS errors configuration mentioned earlier and perform $G = 10000$ simulations. Moreover, it should be mentioned that in order to obtain an insight on the impact of the stochastic modeling information to the standalone INS navigation performance, two 90-second outages were introduced, one that includes straight movement (300-390sec) and one that includes turns (700-790sec).

Now, since the simulator makes certain simplifications (see [28] for more details), the derived solutions cannot provide a realistic representation of a real-life experiment in terms of absolute navigation. On the other hand, a relative comparison in terms of any statistical metric (e.g., empirical coverage, standard estimation error) between the solutions derived when using a different stochastic modeling estimator and for each state, can be utilized for the inference of conclusions regarding
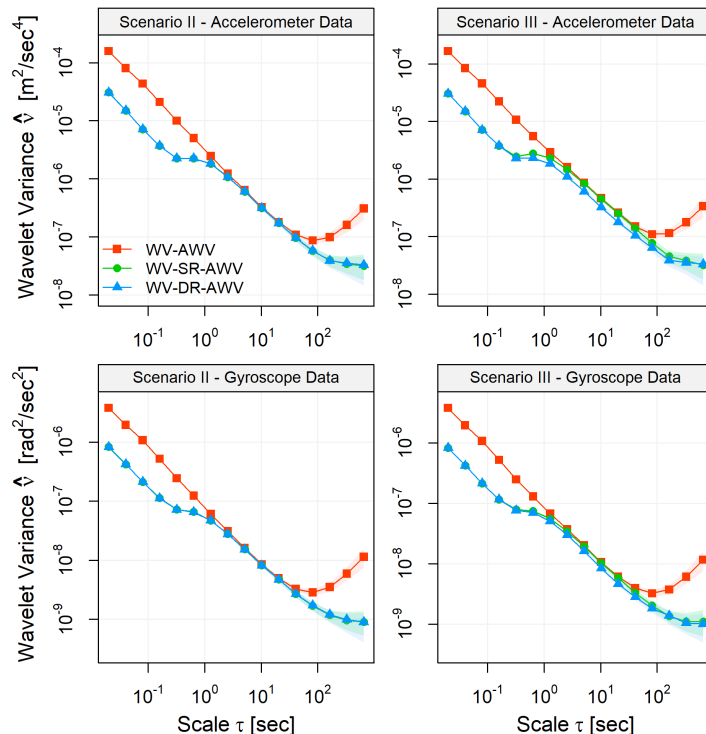
FIG. 6: *WV-AWV, WV-SR-AWV and WV-DR-AWV for the accelerometer data in m^2/sec^4 (top panels) and for the gyroscope data in rad^2/sec^2 (bottom panels) of Scenarios II (left panels) and III (right panels)*

the contribution to the navigation performance of the INS sensor noise stochastic analysis in different contamination scenarios for the calibration data.

Generally, the assessment of any algorithm's performance in the navigation-related literature occurs with a limited number of real-life experiments. However, especially in the case of comparing one stochastic modeling technique over another, these tests cannot realistically be enough in number for the inference of strong statistical conclusions related to their contribution to the overall navigation performance. This is actually the reason why the contribution of the navigation simulator to this study is so important, since it manages to bring together the concept of experimentation and pure statistical analysis.

In our experiments here, and for the purpose of assessing the reliability of the INS standalone navigation performance when stochastic knowledge from each multi-signal (classical and robust) estimator is utilized in the 3 different calibration data contamination scenarios, we chose to investigate the behaviour of the Standard Estimated Errors (SEEs) for the position and orientation states. Moreover, in order to consider the multiple MC realizations produced by the simulator, we average the SEE over the total number G of simulations and create the Averaged Standard Estimation Error (ASEE). However, from an investigation of all the available results, we found that the SEE for all the position and orientation states presents minimal variability from one MC run to another, which means that a smaller number of simulations can be considered for averaging without affecting the derivation of conclusions. Thus, with this in mind, as well as to reduce the computational load, we chose

to use the ASEE quantity based on 100 MC simulations to conduct our study.

What is more, we make a sensible assumption that the AWV-based solution in Scenario I is the optimal one and thus, the validity of the reliability information characterizing other solutions should be evaluated via a comparison with it. Therefore, ratios are evaluated with respect to this reference and for the ASEE (based on 100 MC simulations) information that corresponds to each estimator in the 3 scenarios. For illustration purposes, Fig. 7 is constructed, where a snippet of the ASEE ratios for the East position and roll angle navigation state components are depicted. In addition, the mean values of the ASEE ratio errors during the two GNSS outage regions are calculated as the the difference of each ratio from unity in percentage units and they are provided in Tab. I. Hence, a quantitative analysis of the inspected quantity can be conducted in a straightforward manner.

According to Fig. 7 for Scenario I, the solutions based on the robust estimators for both position and orientation states are characterized by a very similar reliability to the reference. Consequently, the equivalence of the robust multi-signal estimators to the classical one in terms of implied navigation quality is confirmed for the clean calibration data scenario.

Before we move on further, it is important to mention that the goal of robustness in the stochastic modeling of inertial sensor errors is to provide information to the navigation filter that helps the INS performance to remain stable under contamination. Therefore, in the next two scenarios we attempt to assess this while considering a certain mindset. Specifically,
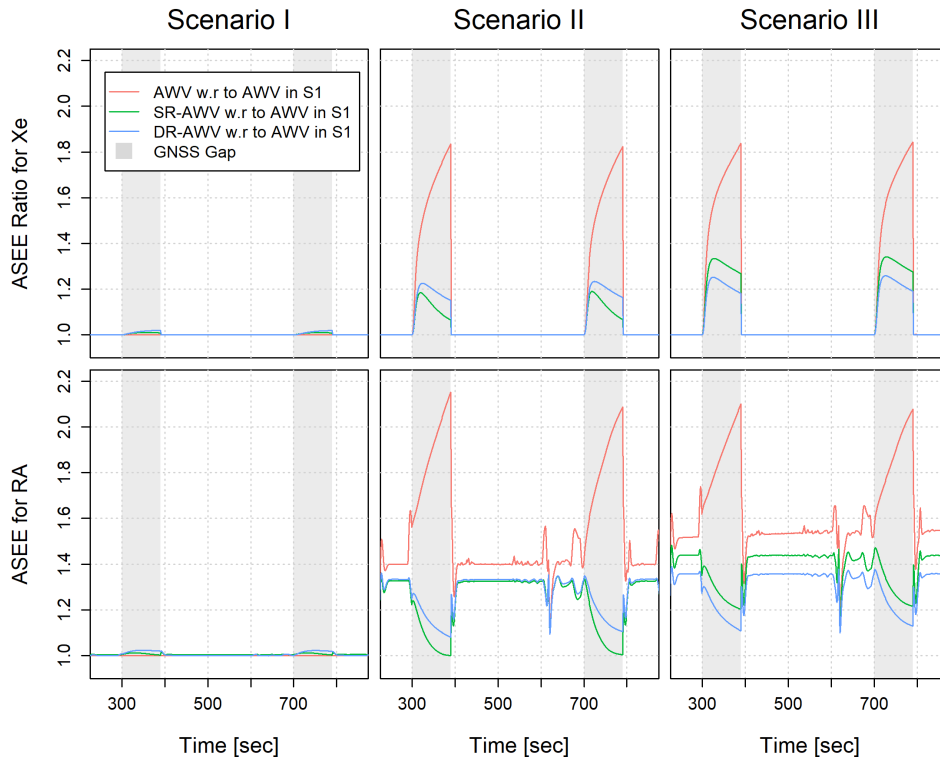
FIG. 7: *ASEE ratios based on 100 simulations for the estimated east position component (Xe) (upper panels) and Roll Angle (RA) orientation component (lower panels). The ratios are between the ASEE of the estimates obtained from the AWV, SR-AWV and DR-AWV estimators in each data scenario relative to the one obtained from the AWV estimator in Scenario I (S1)*

	East position ASEE			Roll angle ASEE		
	AWV	SR-AWV	DR-AWV	AWV	SR-AWV	DR-AWV
	Scenario I (%)					
Outage I	-	**0.96**	1.82	-	**0.74**	2.09
Outage II	-	**0.94**	1.75	-	**0.75**	1.97
	Scenario II (%)					
Outage I	75.07	**9.33**	17.23	95.46	**4.24**	13.01
Outage II	74.05	**9.65**	17.23	91.00	**5.36**	15.46
	Scenario III (%)					
Outage I	76.75	28.88	**20.24**	91.00	25.00	**16.06**
Outage II	77.19	29.72	**21.24**	92.45	26.86	**18.21**

TABLE I: *Mean values of the East position and roll angle ASEE ratio errors for the two GNSS outage regions in each scenario.*

we start by making a realistic assumption that the parameter estimation is stable in the clean scenario. Then, we proceed to investigate how a more stable modeling parameter solution provided by the robust estimators under contamination is translated into the estimation accuracy of the navigation solution as well as what is its relationship with the stable reference solution (derived in the clean scenario).

With this in mind and regarding Scenario II, it is evident from Fig. 7 that the estimations provided by the AWV-driven solution are considerably undermined during the entirety of the trajectory and especially during the GNSS outages. On the contrary, the solutions that encompass the information provided by the robust estimators appear to remain stable, with the SR-AWV providing the most realistic estimation of

confidence by an average margin of approximately 10% for both state types compared to the DR-AWV, according to Tab. I. Furthermore, it should be mentioned that solutions based on the robust estimators appear to provide an equivalent estimation quality during the regions where the GNSS information is available.

Finally, with regard to Scenario III and based on the information conveyed by Tab. I, the solution based on the DR-AWV estimator provides the most realistic uncertainty information. In fact, the ASEE ratio error is only increased by about 3% compared to its respective one in Scenario II for both position and orientation components and each GNSS outage. Inversely, the SR-AWV solution appears to be destabilized since its ASEE ratio error has risen by a margin of about 20% compared to Scenario II. On top of that, and based on Fig. 7, it is worth mentioning that the estimation quality degradation of the SR-AWV solution is present in the entirety of the trajectory, not only during the GNSS outage regions. Therefore, based on our analysis here, it can be inferred that in cases where Scenario II applies, the SR-AWV estimator should be the one chosen for the stochastic analysis of the inertial sensor errors, while in occasions where Scenario III is identified, the DR-AWV is the optimal choice.

VI. CONCLUSIONS

In this paper, we brought forward a robust multi-signal framework for the low-cost and consumer-grade inertial sensor stochastic calibration that is based on the well-established GMWM method and the AWV estimator. Consequently, we

are now capable of efficiently inferring knowledge about the random error behaviour while considering the stochastic parameter variability between replicates and providing safeguards to the estimation process from outliers on two fronts. Moreover, we provided a detailed mathematical reasoning about the conditions that have to be met in order to ensure robustness and statistical consistency.

From this new framework, two estimators were defined and their efficiency in different settings was evaluated and confirmed from two separate aspects. The first was in the context of a simulation setting and in terms of stochastic modeling parameter estimation efficiency in different contamination scenarios. And the latter, was based on stochastically analyzing real data under different contamination scenarios and in turn, investigating the correlation between the quality of the derived knowledge about the inertial sensor errors and the accuracy and stability of the INS/GNSS navigation performance using a navigation simulator. Finally, it is highlighted that the generality of this new method does not limit its application in just the study of the random drift that is displayed by low-cost and consumer-grade inertial sensors. Instead, for example, it could also be used for the random error analysis of GNSS positioning solutions and by incorporating the derived knowledge into the GNSS navigation algorithm, improve the accuracy and stability of its standalone performance.

REFERENCES

[1] D. Titterton, J. L. Weston, and J. Weston. *Strapdown inertial navigation technology*, volume 17. IET, 2004.

[2] G. Huang. Visual-inertial navigation: A concise review. In *2019 International Conference on Robotics and Automation (ICRA)*, pages 9572–9582. IEEE, 2019.

[3] J. H. Wall, D. M Bevly, et al. Characterization of various IMU error sources and the effect on navigation performance. In *Proceedings of the 18th international technical meeting of the satellite division of the institute of navigation (ION GNSS 2005)*, pages 967–978, 2005.

[4] R.O. Allen and D.H. Chang. Performance testing of the systron donner quartz gyro. *Jpl Engineering Memorandum, EM*, pages 343–1297, 1993.

[5] I. Board. IEEE standard specification format guide and test procedure for single-axis interferometric fiber optic gyros. *IEEE Std*, pages 952–1997, 1998.

[6] Y. Yuksel, N. El-Sheimy, and A. Noureldin. Error modeling and characterization of environmental effects for low cost inertial MEMS units. In *Proceedings of IEEE/ION PLANS 2010*, pages 598–612, 2010.

[7] B. Claus. Multiscale statistical signal processing: identification of a multiscale ar process from a sample of an ordinary signal. *IEEE transactions on signal processing*, 41(12):3266–3274, 1993.

[8] R. Johansson, M. Verhaegen, and C. T. Chou. Stochastic theory of continuous-time state-space identification. *IEEE Transactions on Signal Processing*, 47(1):41–51, 1999.

[9] R. H. Shumway and D. S. Stoffer. An approach to time series smoothing and forecasting using the EM algorithm. *Journal of Time Series Analysis*, 3(4):253–264, 1982.

[10] J. Nikolic, P. Furgale, A. Melzer, and R. Siegwart. Maximum likelihood identification of inertial sensor noise model parameters. *IEEE Sensors Journal*, 16(1):163–176, 2015.

[11] Y. Yuksel and H. B. Kaygisiz. Notes on stochastic errors of low cost MEMS inertial units. *línea]. Available: http://www. instk. org/web/static/bibliography/Introduction_to_Sensor_Errors. pdf.[Último acceso: 08 06 2016]*, 2011.

[12] S. Guerrier, J. Skaloud, Y. Stebler, and M.P. Victoria-Feser. Wavelet-variance-based estimation for composite stochastic processes. *Journal of the American Statistical Association*, 108(503), 2013.

[13] D. P Percival. On estimation of the wavelet variance. *Biometrika*, 82(3):619–631, 1995.

[14] Y. Stebler, S. Guerrier, J. Skaloud, and M.-P. Victoria-Feser. Generalized method of wavelet moments for inertial navigation filter design. *IEEE Transactions on Aerospace and Electronic Systems*, 50(3):2269–2283, 2014.

[15] IEEE. Standard specification format guide and test procedure for single-axis interferometric optic gyros. 1998.

[16] N. El-Sheimy, H. Hou, and X. Niu. Analysis and modeling of inertial sensors using Allan variance. *IEEE Transactions on instrumentation and measurement*, 57(1):140–149, 2007.

[17] S. Guerrier, R. Molinari, and Y. Stebler. Theoretical limitations of Allan variance-based regression for time series model estimation. *IEEE Signal Processing Letters*, 23(5):597–601, 2016.

[18] G. Bakalli, A. Radi, N. El-Sheimy, R. Molinari, and S. Guerrier. A computational multivariate-based technique for inertial sensor calibration. In *Proceedings of the 30th International Technical Meeting of The Satellite Division of the Institute of Navigation (ION GNSS+ 2017)*, pages 3028–3038, 2017.

[19] A. Radi, G. Bakalli, S. Guerrier, N. El-Sheimy, A. B. Sesay, and R. Molinari. A multisignal wavelet variance-based framework for inertial sensor stochastic error modeling. *IEEE Transactions on Instrumentation and Measurement*, 68(12):4924–4936, 2019.

[20] G. Bakalli, D. A. Cucci, A. Radi, N. El-Sheimy, R. Molinari, O. Scaillet, and S. Guerrier. Multi-signal approaches for repeated sampling schemes in inertial sensor calibration. *IEEE Transactions on Signal Processing*, 71:1103–1114, 2023.

[21] S. Guerrier, R. Molinari, M.-P. Victoria-Feser, and H. Xu. Robust two-step wavelet-based inference for time series models. *Journal of the American Statistical Association*, pages 1–50, 2021.

[22] M. El-Diasty, A. El-Rabbany, and S. Pagiatakis. Temperature variation effects on stochastic characteristics for low-cost MEMS-based inertial sensor error. *Measurement Science and Technology*, 18(11):3321–3328, sep 2007.

[23] A. Radi, S. Nassar, and N. El-Sheimy. Stochastic error modeling of smartphone inertial sensors for navigation in varying dynamic conditions. *Gyroscopy and Navigation*, 9(1):76–95, 2018.

[24] R. A. Maronna, R. D. Martin, and V. J. Yohai. *Robust Statistics: Theory and Methods*. Wiley, Chichester, West Sussex, UK, 2006.

[25] R. A. Maronna, R. D. Martin, V. J. Yohai, and M. Salibián-Barrera. *Robust statistics: theory and methods (with R)*. John Wiley & Sons, 2019.

[26] D. Mondal and D. B. Percival. M-estimation of wavelet variance. *Annals of the Institute of Statistical Mathematics*, 64(1):27–53, 2012.

[27] F. R. Hampel. The influence curve and its role in robust estimation. *JASA*, 69:383–393, 1974.

[28] Davide A Cucci, Lionel Voirol, Mehran Khaghani, and Stéphane Guerrier. On performance evaluation of inertial navigation systems: the case of stochastic calibration. *IEEE Transactions on Instrumentation and Measurement*, 2023.

[29] F. R. Hampel, E. M. Ronchetti, P. J. Rousseeuw, and W. A. Stahel. *Robust Statistics: The Approach Based on Influence Functions*. John Wiley, New York, 1986.

[30] H. Künsch. Infinitesimal robustness for autoregressive processes. *The Annals of Statistics*, pages 843–863, 1984.

[31] D. A. Cucci, L. Voirol, G. Kermarrec, J.-P. Montillet, and S. Guerrier. The Generalized Method of Wavelet Moments with eXogenous inputs: a fast approach for the analysis of GNSS position time series. *Journal of Geodesy*, 97(2):14, February 2023.

[32] O. Catoni. Challenging the empirical mean and empirical variance: A deviation study. *Annales de l'Institut Henri Poincaré, Probabilités et Statistiques*, 48:1148–1185, 2012.

[33] C. Minaretzis, D. A. Cucci, S. Guerrier, A. Radi, N. El-Sheimy, and M. Sideris. Robust wavelet variance-based approaches for the stochastic modeling of inertial sensor measurement noise. In *Proceedings of the 2022 International Technical Meeting of The Institute of Navigation*, pages 1444–1456, 2022.